

## THE DISK ACCRETION RATE FOR DYNAMO-GENERATED TURBULENCE

AXEL BRANDENBURG,<sup>1</sup> ÅKE NORDLUND,<sup>2</sup> ROBERT F. STEIN,<sup>3</sup> AND ULF TORKELSSON<sup>4</sup>

Received 1995 October 16; accepted 1995 November 4

### ABSTRACT

Dynamo-generated turbulence is simulated in a modified shearing box approximation that removes scale invariance and allows finite accretion rates for a given distance from the central object. The effective Shakura-Sunyaev viscosity parameter,  $\alpha_{\text{SS}}$ , is estimated in three different ways using the resulting mass accretion rate, the heating rate, and the horizontal components of the Maxwell and Reynolds stress tensors. The results are still resolution dependent: doubling the resolution leads to 1.4–1.6 times larger values for the viscosity parameter. For  $63 \times 127 \times 64$  meshpoints we find that  $\alpha_{\text{SS}} = 0.007$ .

*Subject headings:* accretion, accretion disks — hydrodynamics — MHD — turbulence

### 1. INTRODUCTION

Over the last few years it has become clear that a strong candidate for the origin of turbulence in accretion disks is the magnetic shear (or magnetorotational) instability, which is now often called the Balbus-Hawley (1991) instability. In its original form, the instability arises in the presence of a vertical magnetic field, but a purely toroidal field also leads to instability (Balbus & Hawley 1992; Foglizzo & Tagger 1995). The instability continues to operate in the nonlinear regime where the magnetic field is turbulent and mostly in the toroidal direction (Hawley, Gammie, & Balbus 1995; Matsumoto & Tajima 1995). These cases may differ in their stability criteria and the nature of the dominant restoring force (magnetic tension, pressure gradients), but the main mechanism leading to instability is always the same: when two fluid parcels in the same Keplerian orbit are pulled together, they are actually torn apart in the radial direction (due to the change in the centrifugal acceleration). (This is why docking maneuvers in space are difficult.) Once at different radii, and with a magnetic field coupling these otherwise independent parcels, an angular momentum exchange is possible, and energy can be extracted from the shear.

Important outcomes of accretion simulations are the resulting Maxwell and Reynolds stresses, which are expected to be proportional to the gas pressure times a dimensionless number, the Shakura-Sunyaev viscosity parameter. The viscosity parameter can depend on (i) the magnetic field strength, (ii) the pressure, and (iii) the distance from the central object. The dependence on the field strength has been investigated by Hawley, Gammie, & Balbus (1995). It is, however, possible that the magnetic field results from dynamo action (Brandenburg et al. 1995, hereafter Paper I; Hawley, Gammie, & Balbus 1996; Stone et al. 1996). The field strength is then determined by the dynamics and is no longer an independent control para-

meter. The dependence on the pressure is removed by allowing for vertical stratification (Paper I; Stone et al. 1996). In unstratified simulations the vertical extent of the box,  $L_z$ , takes the role of the vertical (Gaussian) pressure scale height,  $H$ , in that both determine the largest length scale of magnetic structures. The models presented by Torkelsson et al. (1995) show that for  $L_z \approx 0.6H$  the unstratified simulations give results for  $\alpha_{\text{SS}}$  similar to the stratified simulations. In this Letter we report preliminary results concerning the dependence on the radius. The main conclusion is that for a finite radius a nonvanishing accretion rate is possible.

### 2. MAKING THE MODEL NONLOCAL

In the local approximation, cylindrical polar coordinates  $(r, \phi, z)$  are replaced by Cartesian coordinates  $(x, y, z)$ , which are valid near a given point  $(R, \phi_0, z)$  with  $x = r - R$  and  $y = r(\phi - \phi_0)$ . Terms of order  $1/R$  are neglected in comparison with  $\partial/\partial x$ . This is, however, invalid for volume-averaged quantities. For example, in the present case, where we assume sliding periodic and periodic boundary conditions respectively in  $x$  and  $y$ , the term  $\langle B_x B_y \rangle / R \neq 0$  is *not* small compared to  $\langle \partial(B_x B_y) / \partial x \rangle = 0$ . (In fact, all averages over  $x$  and  $y$  derivatives vanish.)

It is straightforward to restore all terms of order  $1/R$ . The new set of model equations is formally equivalent to the equations used in Paper I:

$$\frac{\mathcal{D}A}{\mathcal{D}t} = u \times B + \frac{3}{2} \Omega_0 A_y \hat{x} - \eta \mu_0 J, \quad (1)$$

$$\frac{\mathcal{D}u}{\mathcal{D}t} = -(u \cdot \nabla)u - \frac{1}{\rho} \nabla p + g + F + \frac{1}{\rho} J \times B + \frac{1}{\rho} \nabla \cdot (2\nu \rho S), \quad (2)$$

$$\frac{\mathcal{D}e}{\mathcal{D}t} = -(u \cdot \nabla)e - \frac{p}{\rho} \nabla \cdot u + \frac{1}{\rho} \nabla \cdot (\chi \rho \nabla e) + 2\nu S^2 + \frac{\eta \mu_0}{\rho} J^2 + Q, \quad (3)$$

$$\frac{\mathcal{D} \ln \rho}{\mathcal{D}t} = -(u \cdot \nabla) \ln \rho - \nabla \cdot u, \quad (4)$$

where  $\mathcal{D}/\mathcal{D}t = \partial/\partial t + u_y^{(0)} \partial/\partial y$  is the time derivative that includes the transport by the linearized Keplerian shear flow,  $u_y^{(0)}(x) = -\frac{3}{2} \Omega_0 x$ . The full velocity consists thus of the rigid

<sup>1</sup> Nordita, Blegdamsvej 17, DK-2100 Copenhagen Ø, Denmark; after 1996 February: Department of Mathematics and Statistics, University of Newcastle upon Tyne, NE1 7RU, UK.

<sup>2</sup> Theoretical Astrophysics Center, Blegdamsvej 17, DK-2100 Copenhagen Ø, Denmark; and Copenhagen University Observatory.

<sup>3</sup> Department of Physics and Astronomy, Michigan State University, East Lansing, MI 48824.

<sup>4</sup> Sterrenkundig Instituut, Postbus 80000, 3508 TA Utrecht, The Netherlands; after 1995 November: Institute of Astronomy, Madingley Road, Cambridge CB3 0HA, UK.

rotation  $\Omega_0 r$ , the linear shear flow  $u_y^{(0)}$ , and a three-dimensional (turbulent) component  $\mathbf{u}$ . The magnetic field  $\mathbf{B} = \nabla \times \mathbf{A}$  is derived from the magnetic vector potential  $\mathbf{A}$ , and the current density is  $\mathbf{J} = \nabla \times \mathbf{B}/\mu_0$ , where  $\mu_0$  is the vacuum permeability. Gravity in the vertical direction is given by  $\mathbf{g} = -z\Omega_0^2$ , and  $p = (\gamma - 1)\rho e$  is the equation of state for a perfect gas, which is used with  $\gamma = 5/3$ . The microscopic viscosity  $\nu$  enters via the rate of shear tensor  $\mathcal{S}$ . In practice we use instead “numerical” and shock viscosities, but their functional forms are similar. The same applies to the magnetic diffusion term  $\eta\mathbf{J}$ . For further details see Paper I. In this work, the difference lies in the term  $\mathbf{F}$ , which consists of three components:

$$\mathbf{F} = f_\Omega + k_1 f_1 + k_2 f_2, \quad (5)$$

where  $f_\Omega = (2u_y, -\frac{1}{2}u_x, 0)\Omega_0$  (as in Paper I), and the new terms of order  $1/R$  are

$$f_1 = R^{-1} \left( u_y^2 - \frac{B_y^2}{\mu_0 \rho}, -u_x u_y + \frac{B_x B_y}{\mu_0 \rho}, 0 \right), \quad (6)$$

$$f_2 = R^{-1} u_y^{(0)} (2u_y, -\frac{1}{3}u_y^{(0)}, -u_x, 0), \quad (7)$$

which are turned off or on depending on whether  $k_1$  and  $k_2$  equal 0 or 1. These terms result from expressions of the form  $(1/r)(\partial/\partial r)(rB_x B_y)$ , etc., which come from the nonlinear terms such as  $\mathbf{J} \times \mathbf{B}$  and  $(\mathbf{u} \cdot \nabla)\mathbf{u}$ . The importance of these terms has been stressed by Christodoulou, Contopoulos, & Kazanas (1996). Note that we have written out separately the  $u_y^{(0)}$  terms. The contribution  $\frac{1}{3}u_y^{(0)2}/R$  includes the second-order contribution in the expansion of gravity in the radial direction. We retain the shearing box approximation, i.e.,  $\mathbf{A}$ ,  $\mathbf{u}$ ,  $e$ , and  $\rho$  are periodic in  $x$ , but with respect to a time-dependent shift  $\delta y = -\frac{3}{2}\Omega_0 t L_x$ , where  $L_x$  is the extent of the box in the  $x$ -direction. The presence of  $u_y^{(0)}$  in equation (7) breaks the pseudoperiodicity with respect to  $x$  (for  $k_2 = 1$ ), but in practice this contribution is weak and remains unnoticeable in the solution. As in Paper I, we include in some cases a cooling term of the form  $Q = -\sigma_0(e - e_0)$ , which removes the heat generated by viscous and resistive dissipation.

We solve equations (1)–(7) in a box  $|x| < \frac{1}{2}L_x$ ,  $|y| < \frac{1}{2}L_y$ , and  $0 \leq z \leq L_z$ , imposing symmetry conditions at  $z = 0$ . At  $z = L_z$  we impose stress-free, insulating boundary conditions and assume that the magnetic field is vertical. For further details see Paper I. Initially, there is a random seed magnetic field that is needed to get the turbulence going, but this field has zero flux. This gets amplified by dynamo action into a large-scale toroidal magnetic field which changes direction in a cyclic manner with a typical period  $T_{\text{cyc}} \approx 30T_{\text{rot}}$ , where  $T_{\text{rot}} = 2\pi/\Omega_0$ . We cannot rule out that this is a finite size effect which might go away in a truly global model. This field provides a convenient means of estimating the dependence of various transport properties on the mean magnetic field from their mutual correlation.

We performed simulations at two resolutions, comparing results for  $31 \times 63 \times 32$  and  $63 \times 127 \times 64$  meshpoints, using  $R = 10$ ,  $L_x = 1$ ,  $L_y = 2\pi$ , and  $L_z = 2$ . The initial scale height,  $H_0$ , was chosen to be unity, which determines the initial temperature (or internal energy),  $e_0 = \frac{1}{2}H_0^2\Omega_0^2/(\gamma - 1)$ , and the density of the hydrostatic equilibrium  $\rho = \rho_0 \exp(-z^2/H_0^2)$ , where  $\rho_0 = 1$ .

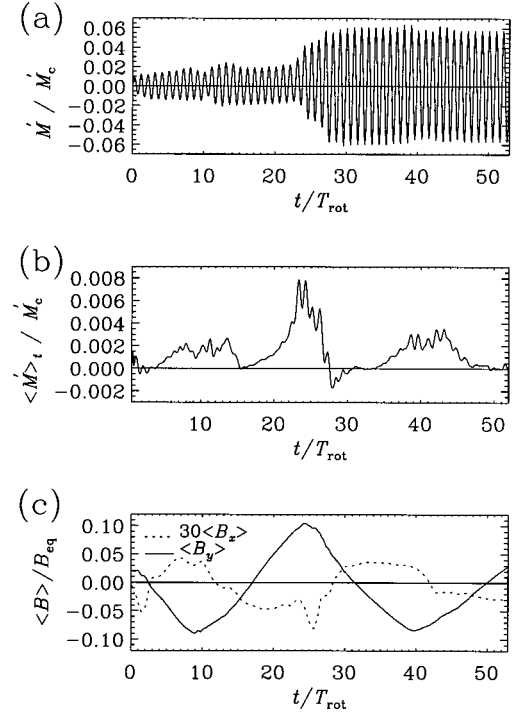


FIG. 1.—(a) Evolution of instantaneous mass flux; (b) running mean of the mass flux; and (c) the mean magnetic field. (The dotted line refers to the radial field, multiplied by a factor of 30.) The scatter shows variations between cycles. (Run A.)

### 3. ACCRETION RATE AND VISCOSITY

We consider the instantaneous mass accretion rate  $\dot{M}$ , which is related to the radial mass flux  $\langle \rho u_x \rangle$  via

$$\dot{M} = -(2\pi R)(2L_z)\langle \rho u_x \rangle, \quad (8)$$

and normalize it by  $\dot{M}_c = 2\pi R \Sigma c_s$ , where  $\Sigma = 2L_z \langle \rho \rangle$  is the vertically integrated average density (which remains constant), and  $c_s^2 = \frac{1}{2}H^2\Omega_0^2 = (\gamma - 1)e$  is the squared isothermal sound speed. Here angular brackets denote volume averages. Note that  $H$  may increase with time (depending on cooling), and we refer to its initial and final values as  $H_0$  and  $H_{\text{max}}$ , respectively. The ratio  $\dot{M}/\dot{M}_c$  corresponds to the Mach number of the accretion flow.

We find that  $\dot{M}$  undergoes epicyclic oscillations with the orbital period,  $T_{\text{rot}} = 2\pi/\Omega_0$ , where  $\Omega_0 = R^{-3/2} = 0.032$  (Fig. 1a). Such oscillations occur also for  $k_1 = k_2 = 0$ , but there the range of  $\dot{M}/\dot{M}_c$  never exceeds  $\pm 0.02$ . More important, the running mean of  $\dot{M}$  taken over one orbit is now positive during periods of high magnetic activity (Figs. 1b and 1c). Indeed,  $\dot{M}$  and  $\langle B_y \rangle^2$  are clearly correlated (Fig. 2). The results for a number of variant models are summarized in Table 1.

In accretion disk theory the accretion rate is related to the turbulent viscosity  $\nu_t$  via the relation

$$\nu_t \Sigma = \dot{M}/(3\pi) \quad (9)$$

(Frank, King, & Raine 1992). Expressing  $\nu_t$  in terms of  $c_s$  and  $H$ , i.e.,  $\nu_t = \alpha_{\text{SS}} c_s H$ , we have

$$\alpha_{\text{accr}} = \dot{M}/(3\pi \Sigma c_s H) = (2/3)(H/R)(\dot{M}/\dot{M}_c), \quad (10)$$

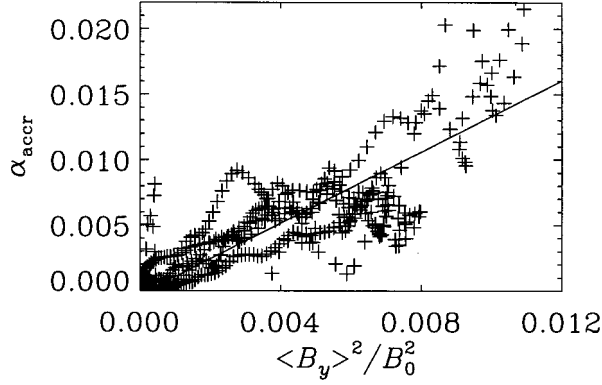


FIG. 2.—Correlation of the viscosity parameter (as derived from the accretion rate) and the mean magnetic field. (Run A.)

where the subscript “accr” refers to how the value of  $\alpha_{SS}$  is obtained. Since  $\alpha_{accr}$  is correlated with the magnetic activity level (Fig. 2), we write

$$\alpha_{accr} = \alpha_{accr}^{(0)} + \alpha_{accr}^{(B)} \langle B_y \rangle^2 / B_{eq}^2, \quad (11)$$

where  $B_{eq} = \langle \mu_0 \rho c_s^2 \rangle^{1/2}$  is the equipartition value based on the thermal energy. The resulting values of  $\alpha_{accr}^{(0)}$  and  $\alpha_{accr}^{(B)}$  are listed in Table 1 for various runs.

*Heating rate.*—In all cases, the disk is heated somewhat initially due to viscous and Joule heating. In particular, when  $\sigma_0 = 0$  (run A), the disk is heated continuously without limit. The rate of heating depends on the turbulent viscosity, since

$$\dot{E} = \nu_t \Sigma \left( r \frac{\partial \Omega}{\partial r} \right)^2, \quad (12)$$

where  $\dot{E} = d\langle \rho e \rangle / dt$  is the average rate of heating integrated vertically over the disk (i.e., multiplied by  $2L_z$ ). Since  $r \partial \Omega / \partial r = -\frac{3}{2} \Omega_0$ , we obtain

$$\alpha_{heat} = \dot{E} / [(\frac{3}{2} \Omega_0)^2 \Sigma c_s H]. \quad (13)$$

This equation is only valid at early times (less than 10–20 orbits) because  $H$  increases with time. The evolution of  $\alpha_{heat}$  and  $\langle B_y \rangle^2 / B_{eq}^2$  is shown in Figure 3a. Note that there is a phase shift:  $\langle B_y \rangle^2 / B_0^2$  leads  $\alpha_{heat}$  by  $\Delta t \approx 1.5 T_{rot} \approx 0.05 T_{cyc}$ . The correlation between  $\alpha_{heat}(t + \Delta t)$  and  $\langle B_y(t) \rangle^2 / B_0^2$  is shown in Figure 3b, and the coefficients  $\alpha_{heat}^{(0)}$  and  $\alpha_{heat}^{(B)}$ , defined by analogy to equation (11), are also listed in Table 1.

*Viscous stress.*—Finally, we estimate the turbulent viscosity parameter directly from the  $(x, y)$ -components of the Maxwell and Reynolds stress tensor,

$$\alpha_{stress} = \langle \rho u_x u_y - B_x B_y / \mu_0 \rangle / (\frac{3}{2} \Omega_0 \langle \rho \rangle c_s H). \quad (14)$$

In Figure 4 we compare the results for runs with different resolution. Note that the higher resolution run (C) gives 1.4–1.6 times larger values of  $\alpha_{SS}$  than the low-resolution runs (B). Likewise, a larger toroidal extent of the box (e.g.,  $L_y = 4\pi$  in run E) also gives rise to larger values of  $\alpha_{SS}$ .

Finally, we make two comments regarding the generated magnetic field. First, we confirm that the kurtosis of the total and toroidal magnetic fields,  $\langle B^4 \rangle / \langle B^2 \rangle^2$  and  $\langle B_y^4 \rangle / \langle B_y^2 \rangle^2$ , respectively, is typically closer to 3 than to 6, indicating that the field is not strongly intermittent (Paper I). Second, the mean toroidal field lags the mean radial field by  $\approx 3\pi/4$  (Fig. 1c). This corresponds to the  $(\langle B_x \rangle, \langle B_y \rangle, 0)$ -vector rotating with the shear.

#### 4. CONCLUSIONS

We have demonstrated that the shearing box approximation, properly modified to include curvature-dependent nonlinear terms, leads to a nonvanishing net accretion flow. The radial mass inflow is dominated by epicyclic oscillations, but its running mean has a positive net value. The turbulent viscosity parameter  $\alpha_{SS}$  inferred from the average mass accretion flow is consistent with the value obtained from the heating rate and the stress. The value of  $\alpha_{SS}$  is still dependent on the resolution and the toroidal extent. The value of  $\alpha_{SS}$  is approximately equal to  $\langle B^2 \rangle / \langle 2\mu_0 p \rangle$  times  $\langle B_x B_y \rangle / \langle B^2 \rangle$ . The results in Table 1 show that the increase with

TABLE 1  
COMPARISON OF VARIOUS MODELS

PARAMETER	RUN					
	O	A	B	C	D	E
Mesh .....	$31 \times 63 \times 32$	$31 \times 63 \times 32$	$31 \times 63 \times 32$	$63 \times 127 \times 64$	$31 \times 127 \times 32$	$31 \times 255 \times 32$
$\sigma_0$ .....	$10\Omega_0$	0	$\Omega_0$	$\Omega_0$	$\Omega_0$	$\Omega_0$
$k_1$ .....	0	1	1	1	1	1
$k_2$ .....	0	0	0	0	1	1
$L_y$ .....	$2\pi$	$2\pi$	$2\pi$	$2\pi$	$4\pi$	$8\pi$
$t_{max}/T_{rot}$ .....	164	52.9	26.4	11.6	19.2	13.3
$H_{max}$ .....	1.1	3.0	1.8	2.0	2.1	1.7
$\langle \alpha_{accr} \rangle$ .....	...	<b>0.004</b>	<b>0.004</b>	<b>0.008</b>	<b>0.005</b>	<b>0.005</b>
$(\alpha_{accr})_{max}$ .....	...	0.025	0.010	0.018	0.018	0.019
$\alpha_{accr}^{(B)}$ .....	...	1.36	0.47	1.8	0.79	1.00
$\langle \alpha_{stress} \rangle$ .....	<b>0.005</b>	<b>0.005</b>	<b>0.005</b>	<b>0.007</b>	<b>0.006</b>	<b>0.006</b>
$(\alpha_{stress})_{max}$ .....	0.018	0.013	0.012	0.012	0.015	0.015
$\alpha_{stress}^{(0)}$ .....	0.002	0.003	0.004	0.005	0.004	0.004
$\alpha_{stress}^{(B)}$ .....	0.029	0.61	0.13	1.51	0.52	0.45
$\langle \alpha_{Maxw} \rangle / \langle \alpha_{Reyn} \rangle$ .....	3.4	3.1	3.1	3.0	2.8	2.7
$\langle B^2 \rangle / \langle \mu_0 \rho u^2 \rangle$ .....	6.2	3.4	3.9	3.1	3.7	3.3
$\langle B^2 \rangle / \langle 2\mu_0 p \rangle$ .....	0.066	0.049	0.037	0.054	0.058	0.059
$\langle B_x B_y \rangle / \langle B^2 \rangle$ .....	0.065	0.087	0.084	0.109	0.089	0.077
$\langle B^4 \rangle / \langle B^2 \rangle^2$ .....	3.0	5.8	3.7	4.7	3.3	3.5
$\langle B_y^4 \rangle / \langle B_y^2 \rangle^2$ .....	2.7	4.2	3.7	3.2	3.2	3.2

NOTE.—The values reproduced in boldface are discussed in the text. The values for the shorter runs (smaller values of  $t_{max}$ ) are uncertain because of insufficient statistics. For run A we find  $\langle \alpha_{heat} \rangle = 0.005$ ,  $(\alpha_{heat})_{max} = 0.023$ , and  $\alpha_{heat}^{(B)} = 1.51$ . In all cases  $\alpha_{accr}^{(0)}$  and  $\alpha_{heat}^{(0)}$  are less than 0.002, except for run C, where  $\alpha_{accr}^{(0)} = 0.006$ .

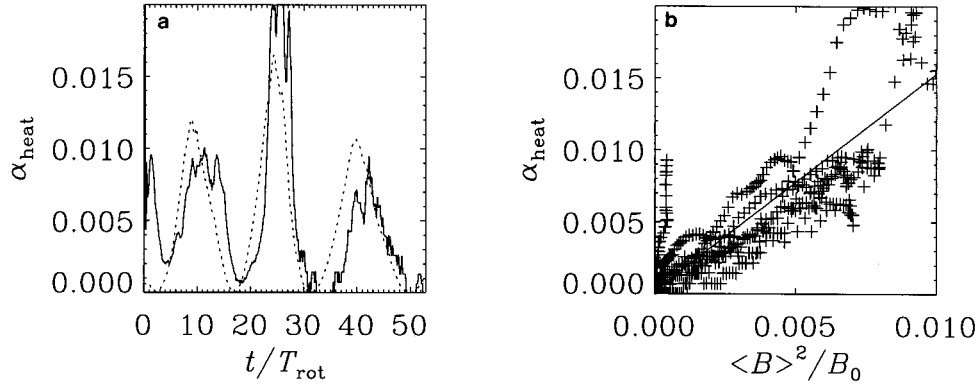


FIG. 3.—(a) Evolution of  $\alpha_{\text{heat}}$  (solid line), compared with  $0.64\langle B_y \rangle^2/B_0^2$  (dotted line). Note the phase shift between the magnetic field and  $\alpha_{\text{heat}}$ . (b) Correlation of  $\alpha_{\text{heat}}$  and  $\langle B \rangle^2/B_0$ . (Run A.)

higher resolution comes mainly from  $\langle B_x B_y \rangle / \langle B^2 \rangle$ . The trend that  $\alpha_{\text{SS}}$  grows with numerical resolution is interesting (see also Terquem & Papaloizou 1996; Ogilvie & Pringle 1996). We will perform additional simulations on finer meshes to determine how much further this trend continues. The inclusion of mass accretion does not significantly affect the values of  $\alpha_{\text{stress}}$ . The contribution from the Maxwell stress is 3 times larger than that from the Reynolds stress, which is also approximately the ratio of magnetic to turbulent kinetic energy.

This work was supported in part by the Danish National Research Foundation through its establishment of the Theoretical Astrophysics Center (Å. N.), NASA grants NAGW 1695, NAG 5-2489 and NAG 5-2218 (R. F. S.), the Stichting voor Fundamenteel Onderzoek der Materie (FOM) and the Nederlandse Organisatie voor Wetenschappelijk Onderzoek (NWO) in the Netherlands (UT). The computations were carried out on the Cray C92 at the Danish computing center UNI●C in Copenhagen.

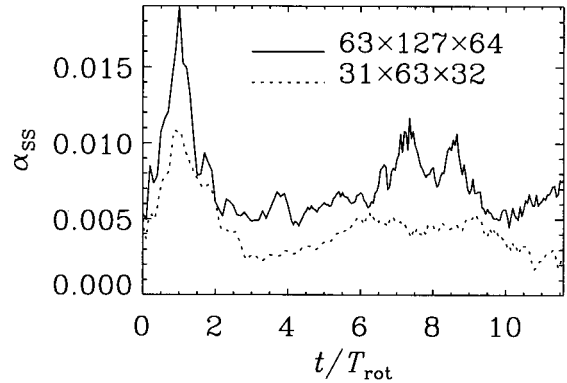


FIG. 4.—Evolution of  $\alpha_{\text{stress}}$  for runs with different resolution. (Runs B and C.)

#### REFERENCES

- Balbus, S. A., & Hawley, J. F. 1991, *ApJ*, 376, 214  
 ———. 1992, *ApJ*, 400, 610  
 Brandenburg, A., Nordlund, Å., Stein, R. F., & Torkelsson, U. 1995, *ApJ*, 446, 741 (Paper I)  
 Christodoulou, D. M., Contopoulos, J., & Kazanas, D. 1996, *ApJ*, in press  
 Foglizzo, T., & Tagger, M. 1995, *A&A*, 301, 293  
 Frank, J., King, A. R., & Raine, D. J. 1992, *Accretion Power in Astrophysics* (Cambridge: Cambridge Univ. Press)  
 Hawley, J. F., Gammie, C. F., & Balbus, S. A. 1995, *ApJ*, 440, 742  
 Hawley, J. F., Gammie, C. F., & Balbus, S. A. 1996, *ApJ*, in press  
 Matsumoto, R., & Tajima, T. 1995, *ApJ*, 445, 767  
 Ogilvie, G. I., & Pringle, J. E. 1996, *MNRAS*, in press  
 Stone, J. M., Hawley, J. F., Gammie, C. F., & Balbus, S. A. 1996, *ApJ*, submitted  
 Terquem, C., & Papaloizou, J. C. B. 1996, *MNRAS*, in press  
 Torkelsson, U., Brandenburg, A., Nordlund, Å., Stein, R. F. 1995, *Astrophys. Lett. Commun.*, in press